Understanding the optical spectroscopy of amphiphilic molecular rectifiers: A density functional approach

Osbert Tan, S. J. Clark,[a] M. Szablewski, and G. H. Cross
Department of Physics, University of Durham, South Road, Durham DH1 3LE, United Kingdom

(Received 12 May 2010; accepted 25 October 2010; published online 23 December 2010)

We present results of first principles density functional theory calculations of the electronic and atomic structural properties of model Z-type Langmuir–Blodgett (LB) layers comprising amphiphilic quinolinium tricyanoquinodimethanide (Q3CNQ) chromophores. We find that the chromophore electronic ground state is not as clearly "zwitterionic" as required by models to explain electrical rectification purportedly seen in such systems. The computed visible region transitions are not what have been assumed to be the intervalence charge transfer bands seen in the visible region of molecules in Z-type LB films. Our own LB deposition and spectroscopic studies suggest that almost all visible region features previously seen may be ascribed to aggregates. The calculated lowest energy electronic excitation between HOMO and LUMO levels, which is located in the near infrared region, has a transition moment aligned approximately 9° off the molecular long axis, and has a normalized oscillator strength of 1 order of magnitude higher than those of the visible region transitions. This most dominant feature has been neglected from discussions of Langmuir–Blodgett layer rectification but our own deposition studies show no sign of this feature, indicating that the structure of the modeled system differs from that of typical experimental structures. The model indicates that such idealized LB layer structures cannot confidently be invoked to explain their experimental optical or electrical properties. © *2010 American Institute of Physics*. [doi:10.1063/1.3516177]

I. INTRODUCTION

Unimolecular rectifiers have received intensive research attention over many years because of their application potential in organic nanocomputers.[1–4] The long chain quinolinium tricyanoquinodimethanide (Q3CNQ) molecule (typically $C_{16}H_{33}$–γQ3CNQ) is of special interest as it is the first experimentally reported example of a current rectifier when arranged as a multilayer Langmuir–Blodgett (LB) film.[5,6] The molecule is often claimed to possess the D^+–π–A^-↔D^0–π–A^0 (D—electron donor, A—electron acceptor, π—conjugated π bond link; superscripts indicate charge polarity) resonance structure suggesting that it is the asymmetry of the electronic density that is the origin of molecular rectification. The ground state is commonly regarded as "zwitterionic" with a nonzero dihedral twisting angle between the donor and acceptor aromatic ring planes. The rectification mechanism for $C_{16}H_{33}$–γQ3CNQ LB films sandwiched between two identical metal electrodes has been interpreted in terms of a modified Aviram and Ratner model,[7] where the interlayer electron transport is achieved by the electric-field driven excitation from D^+–π–A^- ground state to the D^0–π–A^0 first excited state, followed by electron transfer across the two molecule–metal interfaces. However, the requirement for electron transfer across the insulating long chain hydrocarbon layer still remains a problematic area for discussion since electronic coupling between any two LB layers is thought to be extremely small and would not favor intermolecular charge transfer.[8] This problem lies unresolved at the heart of current understanding of the rectifying properties of this molecule. Alternative interpretations[9] offer the conclusion that $C_{16}H_{33}$–γQ3CNQ cannot be called a "molecular rectifier," but rather a "directional insulator."

As often described in experimental reports, the UV-visible absorption spectra of C_nH_{2n+1}–γQ3CNQ LB multilayers are regarded as key to the description of the electronic structure of the chromophores within the LB molecular stack. A survey shows that it has been impossible to reach a consistent set of results for LB films of this family and many observations still lack a clear interpretation as we now summarize. For example, the optical absorption features and optical nonlinearity (second harmonic generation, i.e., SHG).[10–12] of LB films of long chain Q3CNQ homologues have been found to be markedly different from those of the short chain homologues. A visible region absorption band is seen at 563 nm for long chain homologue LB films whereas the band lies at 614 nm for short chain homologues; SHG signals from the long chain homologue LB films are fairly large but are nearly absent for short chain Q3CNQ homologues. As an attempt at explanation, these phenomena are thought to be due to the dimerization of the short chain Q3CNQ at the air–water interface before being transferred onto the solid substrate, giving rise to a centrosymmetric structure (zero SHG) and a concomitant red shift of the transition energy in LB films. The long chain Q3CNQ homologues, by contrast, are expected to give a normal parallel monomolecular "Z-type" (noncentric) multilayer configuration. On this basis the 563 nm band would therefore be entirely attributable to the visible region transition properties of the monomeric Q3CNQ chromophore. Further observations report that two different

[a]Author to whom correspondence should be addressed. Electronic mail: s.j.clark@durham.ac.uk.

phases of long chain Q3CNQ ($C_{16}H_{33}$–γQ3CNQ) LB films result from different concentration ranges of the spreading solutions. These LB phases are characterized by having the 563 ± 5 nm band and finite second-harmonic signals as before but the two concentration regimes produce layers that have either 8° ($c \geq 0.02$ mg ml^{-1}) or 24° ($c \leq 0.01$ mg ml^{-1}) molecular axial average tilt angles from the surface normal. The physical reason for how and why these differences of concentrations in spreading solutions should lead to such a disparity of molecular tilt angles in LB phases remains unclear. Furthermore higher concentrations of spreading solutions[13] give LB films with a band at 610 nm in comparison with the 563 ± 5 nm band in the same molecular films produced from more dilute solutions. Some differences seem to depend on whether the layer is a multilayer or monolayer. Based again on spectroscopic studies, a sharp CT band at 570 nm was originally observed for an 11-layer LB film of $C_{16}H_{33}$–γQ3CNQ transferred onto quartz.[7] However, the monolayer of the same molecule on quartz gives only a very weak and hardly observable absorption maximum centered at 565 nm.[14] This is at odds with more recent work where the polarized absorbance spectrum indicates that a 14-layer $C_{16}H_{33}$–γQ3CNQ film transferred onto quartz has a band at 530 nm with transition moment along the surface normal,[15] when the LB film is deposited at a pressure reasonably below the isotherm collapse point.

In all of these very diverse cases, the assumption has been that the band in the midvisible region of the spectrum is the lowest energy electronic excitation for the chromophore and that its position can be ascribed to hyposochromism from the solution phase position due to the preferred stabilization of the charge-separated ground state over the less polar excited state in higher polarity surroundings. In other words, the ground state is taken to be a polar state, often referred to as a "zwitterionic" state and it is possibly assumed that the condensed LB film provides the polar environment required for such a blue shift. In this paper we are suggesting the possibility that the visible transitions seen experimentally in LB films can be mistaken for intramolecular charge transfer (CT) excitations between these two purported states and, furthermore, reporting the possibility that the polarity of the LB film environment can, in fact, stabilize a ground state that is less polar than the vacuum or solution state. This, by contrast, would present as a bathochromic shift of the lowest energy CT transition. That such a feature has been unreported to date, coupled with the first cautionary note, may help to explain some of the reported inconsistencies. Noting this we do acknowledge that the requirement for these conditions would be that one is able to deposit a well ordered Z-type molecular multilayer that forms a crystal phase of the type examined by our density functional theory (DFT) work herein.

Theoretical studies of the Q3CNQ electronic spectrum hitherto have been confined to conventional semiempirical methods. AM1/CI and PM3/CI theories have been previously used to compute the absorption spectra for several molecular conformations.[8,16] Nevertheless, these calculations are somewhat restricted to the single isolated molecule and less attention is paid to local environmental effects, particularly for the molecule in its LB film state.

To take account of the local environmental influence on the optimal state of charge distribution and the optimal molecular structure conformation, an improvement is possible in which a two-state Mulliken model is constructed to describe the molecular Hamiltonian[17,18] and the problem of the equilibrium molecular geometry is resolved by introducing Holstein coupling.[19,20] This gives a good simulation for solution spectra and the Q3CNQ ground state is clearly identified in this scheme as zwitterionic; showing inverse solvatochromism (transition energy lowering with lower polarity of solvents). The simulated LB film spectrum, however, is proposed to derive from a model in which a rough lattice structure is presumed and calculated for a finite size. The absorption spectra peaked between 550 and 570 nm thus calculated is based on molecular parameters extracted from solution spectra and, importantly, is taken to arise from a perturbation of the same two and only states considered in this method.

In order to address the disparities in experimental reports and to improve on the solid-state theoretical approaches we now offer our theoretical analysis. We present an *ab initio* DFT study of the Q3CNQ molecule with a long hydrocarbon chain ($C_{18}H_{37}$–γQ3CNQ) built into an LB film to circumvent the need for semiempirical assumptions of the previous methods. In our model, the Z-type multilayer LB film is presumed to comprise an infinite number of triclinic unit cells, each molecule built in one unit cell to complete a quasicrystalline structure. Here the compromise has to be made that our LB crystal structure is rigid; a situation unlikely to be realized in experiment since molecules in the film can explore the many possible relaxation degrees of freedom. In particular, the rotational freedom around the molecular long axis is not a feature of such an idealized structure and thus the simulation is that of complete azimuthal plane anisotropy in the repeatingunit cell configuration, as in a perfect crystal. Nevertheless, since experimental interpretations are often based on the idea of some orientational polar order and a condensed phase, it is useful to explore this idealized system and to compare predicted with observed spectroscopic effects.

II. COMPUTATIONAL DETAILS

All calculations are performed with the planewave pseudopotential implementation of DFT using the CASTEP code.[21,22] A planewave basis set is used to expand the valence electron wavefunctions; the cut-off energy is chosen to be 400 eV which we find converges total energy differences to better than 1 meV/atom. The Perdew–Burke–Ernzerhof (PBE) (Ref. 29) functional describes the many-electron exchange-correlation interactions for structural determination; and ultrasoft pseudopotentials are employed to account for the core. We apply the Monkhorst–Pack (MP) *k*-point sampling scheme to perform the integration over the first Brillouin zone to calculate the total electron density as well as the Kohn–Sham (KS) orbitals. The grid (detailed in each case below) is set to converge total energy differences similar to that for the plane wave cut-off. We use the Pulay density-mixing scheme to minimize the total KS energy which is considered converged when energy differences are smaller than 2×10^{-6} eV/atom. The molecular geometry and lattice

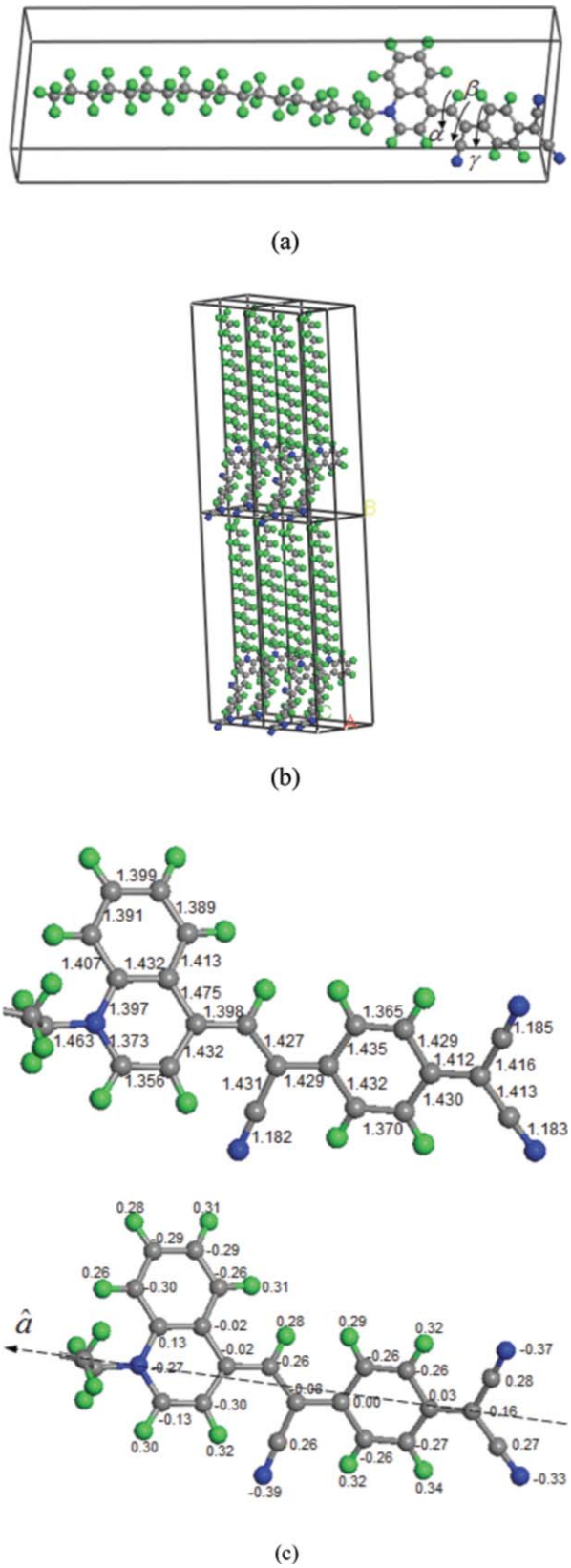

FIG. 1. (a) The optimized geometry of the $C_{18}H_{37}$–γQ3CNQ molecule built in the unit cell of the LB multilayer; α, β and γ are three dihedral twisting angles in the π-bridge region. (b) The constructed Z-type multilayer structure of the LB film. (c) The calculated bond lengths of the Q3CNQ chromophore in the LB lattice structure. The Mulliken charge distribution is also shown with the molecular long axis, $\hat{a}$, superimposed and defined as a vector connecting the quinolinium nitrogen and methylene carbon coordinate positions.

structure optimization is implemented by the Broyden–Fletcher–Goldfarb–Shanno (BFGS) algorithm to minimize the enthalpy, which allows the minimization of the force on atoms and the stress in the unit cell simultaneously.[23] The maximal ionic force and the maximal stress component are set to be 0.05 eV/Å and 0.1 GPa, respectively, in the convergence. The electronic charge density, KS orbitals, and atomic positions were then used to calculate a number of material properties as discussed below. Furthermore, the semilocal nature of the PBE exchange-correlation functional does not allow for a good description of some states, for example, there is an increase in the delocalization of the electron density in π-conjugated materials and the optical band gap is also underestimated. Therefore, for considering the optical spectra, we use the nonlocal screened exchange functional (described below) that has been shown[30] to improve on the standard semilocal functionals for excitation energies.

III. SIMULATION RESULTS

A. Molecular structure and charge distribution in the LB multilayer

The optimized $C_{18}H_{37}$–γQ3CNQ molecular geometry and the associated LB lattice structure are shown in Figs. 1(a) and 1(b), respectively. The in-plane molecular area, defined as the minor area of the parallelogram shown in Fig. 1(a), is calculated to be 41 Å^2. This is in reasonable agreement with the experimental molecular area of 48 Å^2 at the deposition pressure 28 mN/m at 17 °C,[15] but in much better agreement with the molecular area of 40Å^2 at the collapse point on the experimental LB monolayer isotherm. Additionally, the computed in-plane 2D molecular repeating distance (5.4 Å × 9.7 Å) is quite close to that of the deposited LB monolayer observed by STM,[7] which is reported to be 6 × 12 Å.

The dihedral twist of Q3CNQ in the LB phase is often discussed as having a significant role in the determination of the molecular charge transfer state. The calculated dihedral twisting angles in the Q3CNQ optimized molecular conformation are shown in Table I. The total twisting angle between the donor and acceptor aromatic planes is obtained by summing up the three dihedral twisting angles. As shown, the predicted large twisting angle of 35.2° in the LB phase can be seen to come from steric hindrance as well as the dipolar interaction in the molecular array; it agrees very well with the measured twist angles of Q3CNQ and related analogues in the crystalline structure.[24] Forexample, the twist angle

TABLE I. Dihedral interplane twisting angle (in degrees) of the optimized geometry of $C_{18}H_{37}$–3CNQ in the LB multilayer structure in the isolated state.

Dihedral twisting angle (deg)	LB multilayer structure	Single molecule
α	14.629	– 7.432
β	14.753	3.202
γ	5.803	9.646
Total angle	35.185	5.416

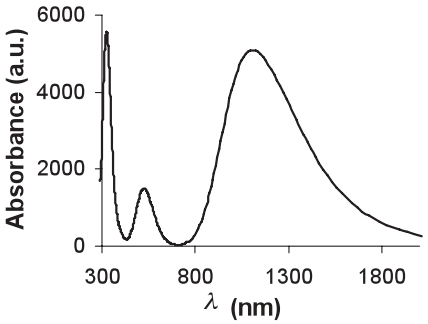

FIG. 2. Simulated absorption spectra of $C_{18}H_{37}$–γQ3CNQ in the multilayer LB film after band gap correction as discussed in the text.

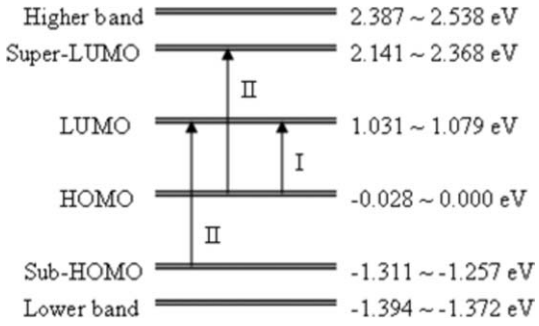

FIG. 3. Computed Q3CNQ LB film energy level structure (from the PBE functional) near the HOMO and LUMO levels. Roman numeral "I" represents the principal transition corresponding to the absorption band in the near-infrared region, and II represents the secondary transitions corresponding to the visible absorption band. The bands below sub-HOMO and above super-LUMO (only two are representatively shown here) are quite close to each other by having much smaller energy difference.

of α-P3CNQ (α-picolinium tricyanoquinodimethanide) is determined to be[25] 30.1°, while that of $C_{10}H_{21}$-αQ3CNQ (decyl-α-quinolinium tricyano-quinodimethanide) is identified as[26] 31.4°. Note that in the isolated state, the molecule relaxes to a configuration that is approaching coplanarity. The total dihedral angle between donor and acceptor planes reduces to only 5.4°.

The bond lengths of $C_{18}H_{37}$–Q3CNQ in the Z-type LB film unit cell are given in Fig. 1(c). The bond length pattern shows evidence of a mixed ground state. In particular, the two short C–C bonds (1.365 and 1.370 Å) in the acceptor ring system are those expected for the quinonoid form and in the quinolinium (donor) ring system, we see a single short C–C bond (1.356 Å) where we would place a double bond in a quinonoid resonance form. However, a calculation of the Mulliken charge distribution on the dicyanomethanide tail shows the presence of a total net (sum of Mulliken charge over the five atoms comprising the group) charge of about −0.3 eV and indicates a partially zwitterionic ground state (note that x-ray photoelectron spectroscopy evidence[14] and the reflection–absorption infrared spectroscopy evidence[27] corroborates this finding). Importantly, we calculate the molecular dipole moment from the Mulliken charge distribution to be 15.9 D. This is considerably smaller than measured in any solution study and smaller than theoretical calculations for the vacuum state (19.2 D, see Appendix) or solvated molecule.

B. Electronic properties

The optical absorption spectrum of $C_{18}H_{37}$–γQ3CNQ in the LB multilayer structure is calculated via Fermi's golden rule based on the optimized electronic structure in the optimized geometry, as shown in Fig. 2.

The converged k-point MP grid is 6×6×3.The incident light propagation direction is prescribed to be along the surface plane normal with no polarization preference, in order to calculate all the in-plane transition moments under the constrained conditions of molecular orientational anisotropy. This is a reasonable simulation of the experimental condition[15] where polarized light is used to perpendicularly irradiate a film where free rotation around the molecular axis should, in the absence of macroscopic azimuthal alignment, produce in-plane optical isotropy. We adopt a band gap correction scheme that enhances the calculated KS gap in order to compensate for the underestimation of the true fundamental gap due to the neglect of the derivative discontinuity in the local exchange-correlation functional (the PBE functional) with respect to the particle number. A nonlocal screened Hartree–Fock XC-functional is used to evaluate the energy levels, and this yields a 0.16 eV enhancement to be added to the original band gap energy calculated from the PBE functional. Note that the screened exchange functional has recently been shown to give a good description of excitation energies in the solid state.[30] Most distinctive in the spectrum of course is the very prominent absorption band extended into the near-infrared region centered around 1150 nm, which has to our knowledge not been reported in any experimental result except perhaps hinted at in one case where a slight shoulder at the base of the visible band on the long wavelength side was observed for long chain Q3CNQ LB film spectra.[28] The visible region band of centre wavelength 532 nm (equivalent to 2.33 eV) is a much weaker transition and is well above the energy of the transition between HOMO and LUMO levels according to the computed band structure shown in Fig. 3. This band is clearly associated with the energy differences between the HOMO and super-LUMO as well as between the sub-HOMO and LUMO levels. The transition band at 324 nm in the optimized simulated absorption spectrum (corresponding to 3.83 eV in energy) is identified with a transition from the occupied lower energy bands to the higher conduction bands, comprising many transition possibilities and therefore will be seen as an optically isotropic transition. As reported in experiments, the absorbance of this prominent high energy peak is unchanged in angle-dependent spectroscopy.

Because of the focus on polarization studies of the visible band absorption properties in previous studies, we look closely at the computed transition moments and their projection onto the experimental reference frame. The chromophore orientation in the LB lattice structure (vector $\hat{a}$ determined from atomic positions) can be estimated to be 33° tilted from the surface normal. The alkyl chains are aligned to the surface normal. Note that this calculated chromophore tilt angle is reasonably close to the whole molecule (chromophore plus chain) average tilt angle to the normal of 29° determined from spectroscopic ellipsometry for C_{16} homologue films

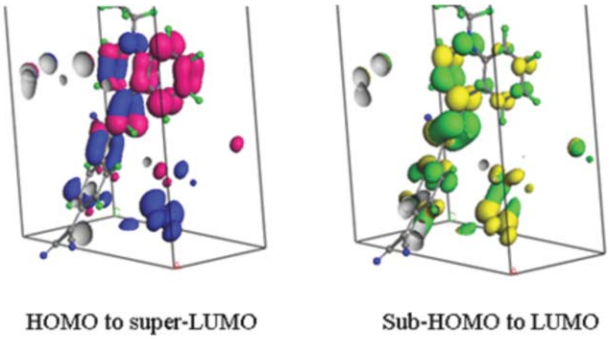

(a)

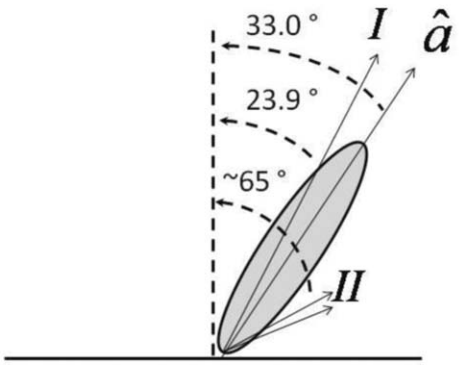

(b)

FIG. 4. (a) Kohn–Sham HOMO (blue) to super-LUMO (pink) and Sub-HOMO (green) to LUMO (yellow) electron density distributions of the $C_{18}H_{37}$–γQ3CNQ chromophore in the modeled LB layer. (b) Schematic representations of the chromophore axis and the major transition moments onto the layer plane normal. The direction and relative magnitudes of the transition moments are schematic but indicate relative scales.

transferred above the collapse pressure, where a midvisible band at 570 nm, polarized fully in the LB film plane was previously observed.[15]

The electron density distribution shifts for these two secondary transitions (HOMO to super-LUMO and sub-HOMO to LUMO) are illustrated in Fig. 4(a). What is immediately apparent is that neither of these transitions involves significant electron density transfer along the molecular long axis. The optical matrices are computed and are calculated at each k point in the MP grid between the relevant transition energy levels and only the matrix corresponding to the minimum energy difference between two bands in k-space is selected, since that is where the transition is most likely to take place. The diagonalized optical transition matrix of the HOMO to super-LUMO transition is given as (0.0573, 0.0376, and 0.0992) with the normalized oscillator strength calculated as 0.0165, and that of sub-HOMO to LUMO as (0.1124, 0.0510, and 0.0492) with normalized oscillator strength 0.0194. These two secondary transitions are therefore comparable in strength to each other and we can deduce that the tilt angles of moments from the surface normal are 68.8° for HOMO to super-LUMO and 60.4° for sub-HOMO to LUMO. We have resisted throughout this paper referring to the visible region band as the intramolecular charge transfer (ICT) band as this evidence now suggests that in the case of ideal Z-type layers any visible region features corresponding to intramolecular transitions are clearly not those associated with a $D^+-\pi-A^- \leftrightarrow D^0-\pi-A^0$ resonance. The near-infrared band on the other hand has an optical transfer matrix given by (0.2005, 0.3423, and 0.0571) and normalized oscillator strength of 0.1606. This transition is aligned at 23.9° to the surface normal, which means that it makes an angle of 9.1° to $\hat{a}$ as we have chosen to define it in Fig. 1(c). It is this band that can be defined as the ICT band (or "IVT" band[14]) in the modeled structures.

Since all the calculations obtained above are for the electronic structure in one unit cell comprising a single molecule, a $C_{18}H_{37}$–γQ3CNQ dimer supercell in an LB multilayer structure was also constructed to recompute the absorbance spectrum and orbitals to examine the possibility of intermolecular electron transfer behavior, as purported by many previous experimental observations.[11,12] From the calculation results, the charge transfer is found to be confined to individual chromophores and no intermolecular orbital crossover can be detected. The calculated absorbance spectrum from the dimer supercell gives exactly the same absorption features as that from the single unit cell. We thus conclude that there are no intermolecular charge transfer transitions in the long chain Q3CNQ LB multilayer configuration when arranged according to our model. This is not to say of course that dimer and larger, aggregates do not form in experimental LB films.

IV. EXPERIMENTAL STUDY

Solutions of $C_{18}H_{39}$Q3CNQ (synthesized in accordance with procedures outlined in Ref. 12) were prepared at a weight concentration of 0.05 mg/ml in Sigma-Aldrich HPLC grade dichloromethane by sonication at room temperature until no particles were visible to the naked eye. The solutions were used either as prepared or after filtering through a 0.2 μm Millipore filter. Spectroscopic study of the filtered and unfiltered solutions showed no difference in the position of a strong absorption band centred at 820 nm although a noticeable reduction in relative absorbance strength was noted for the filtered solutions. The spectra were in complete accordance with all available previous reports. Solutions were applied to a pure water subphase (18 MΩ) (purified by means of an Elga Option 3 water purifier equipped with a UHQ ultrapure water unit) the ambient subphase acidity of which was measured as pH6. LB film deposition was carried out on a circular Nima Technology alternate layer trough. The subphase was allowed to cool to room temperature once it had been transferred into the LB trough. Sixteen hundred microliters of the dichloromethane solution of $C_{18}H_{39}$–γQ3CNQ was deposited onto the subphase surface dropwise by means of a Hamilton micro syringe, (onto one compartment of the trough only). After evaporation of the solvent (15 min), compression was undertaken at 50 cm^2/min under pressure control, until a pressure of 25 mN m^{-1} was attained. Cleaned (hydrophilic character) glass microscope slides (RS France ISO 8037) were dipped through the clean water surface in the other compartment and up through the compressed floating monolayer at 4 mm/min in order to deposit in a Z-type manner.

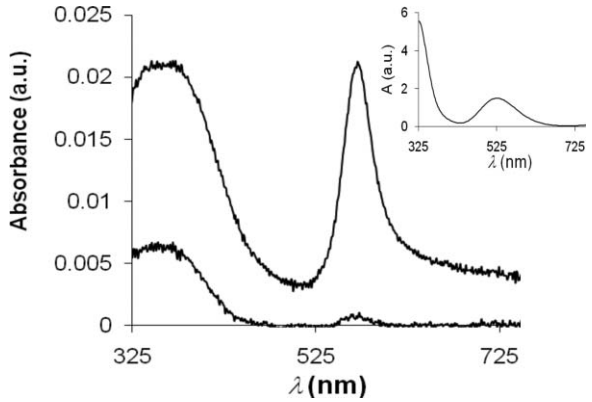

FIG. 5. Experimentally determined absorption spectra of Z-type LB layers of $C_{18}H_{39}$–γQ3CNQ. Upper trace; Z-type bilayer produced from a compressed film obtained from an unfiltered solution. Lower trace, monolayer produced from a filtered solution. (Inset) Theoretical absorbance spectra of the corresponding wavelength region using the 0.16 eV bandgap correction data of Fig. 2.

The absorbance spectra of a monolayer obtained from a filtered spreading solution and a bilayer obtained from an unfiltered spreading solution are shown together in Fig. 5. Spectra were taken out to 1800 nm but no measurable absorption features were seen. The inset of Fig. 5 shows that we can expect in an ordered layer system the absorbance strength of the midvisible band (around 532 nm) will be substantially lower than the short wavelength feature around 320 nm. This is reflected in the experimental absorbance spectra of the film obtained after solution filtering. By contrast, the film obtained from unfiltered solution has a midvisible peak (at 570–580 nm) of almost the same absorbance value as that at 360 nm. Furthermore, we note a discrepancy between the two in that the relative absorbance of the 570–580 nm feature does not scale at all with layer thickness. The bilayer absorbance value is approximately 53 times that of the monolayer, however, the short wavelength features are more rational, the feature from the "filtered" bilayer being around three times as strong as the "unfiltered" monolayer.

Clearly we can propose that the midvisible feature is extrinsic to the features expected of an LB layer system ordered as we describe in the DFT model. Furthermore, we can propose that aggregates larger than 0.2 μm in the spreading solution confer the spectral property seen between 570 and 580 nm and that we might expect that the strength of this feature is related in some way to the concentration of these aggregates in the spreading solution. Only by undertaking some rather surprisingly coarse filtering of the spreading solution we can find spectra that begin to resemble the ideal modeled LB layers. However, this argument only applies to the visible region because in none of our studies have we seen the near-infrared feature that is predicted by our detailed DFT study.

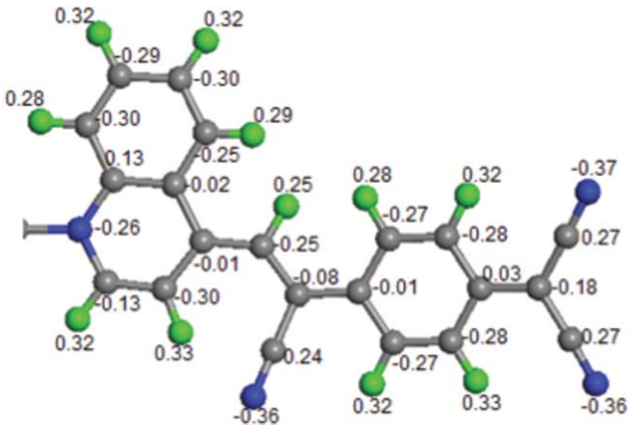

FIG. 6. Mulliken charge distribution of the Q3CNQ chromophore group of the molecule in the isolated state.

V. CONCLUSIONS

We have shown that in a model Z-type multilayer of the long chain Q3CNQ molecule ($C_{18}H_{37}$–γQ3CNQ in this paper), the lowest energy HOMO–LUMO transition (CT) state lies in the near-infrared region of the spectrum. This can be viewed as a red shift of the band centred near 800 nm, which appears in solutions with low polarity solvents such as chloroform or dichloromethane. The visible region transition in this model system is only a rather weak feature and comprises a mixture of transitions that are directed off-axis and are not connected with the observations most often seen in experiments. The dipole moment of the molecule in the layer, calculated to be 15.5 D, prompts us to regard the ground state as tending toward the neutral (quinonoidal) geometry, rather than the polar (zwitterionic) geometry often proposed in experimental work. It seems therefore that interpretations of experimental data cannot be made in terms of the model Z-type multilayer or monolayer structure. The origin of the strong visible region features seen in experiment remains obscure. The previous evidence that is often contradictory from study to study implicates experimental artefacts whose origins are unidentified. Our contribution to this has been to show that we achieve some consistency of results if we simply filter the Langmuir layer spreading solutions before applying them to the subphase. Unfiltered solutions give strong sharp visible region features that accord with previous work, whereas filtered solutions give layers with almost featureless visible absorbance. In none of our studies and in none of any of the previous work, do we find evidence of the strong near-infrared band predicted here. Given this evidence, future work therefore might be directed at a theoretical understanding of the electronic structure and optical properties of arbitrary molecular condensates (aggregates) and would be a challenging exercise.

ACKNOWLEDGMENTS

One of us (O.T.) is grateful to the UK Engineering and Physical Sciences Research Council and to the Farfield Group Ltd. for a Marie Curie Industrial Studentship.

APPENDIX: MOLECULAR STRUCTURE AND CHARGE DISTRIBUTION *IN VACUO*

To compare the calculation method with previous results and to provide a comparison with the LB condensed phase we perform a computation to optimize the geometry of

$C_{18}H_{37}$–γQ3CNQ in the isolated (vacuum) phase by putting the molecule into a unit cell large enough so that the interactions from neighboring molecules can be neglected. The lattice parameters are therefore set to be 10 Å larger than those in the LB solid phase, and set to be $15.4 \times 19.7 \times 45.5$ Å. The scale of the lattice parameter extension is empirically selected from which a good convergence of the molecular conformation can be visualized to well approximate the vacuum space. A $2\times1\times2$ *k*-point mesh is used to achieve self-consistency.

The calculated individual and total dihedral twisting angles are displayed in Table I where we see that the molecule is almost planar. According to a calculation of the Mulliken charge distribution in the isolated phase (Fig. 6) we calculate a vacuum state dipole moment of 19.2 D, which is around 4 D larger than that calculated in the LB multilayer model. The depolarizing net local field in the LB film condensed phase comprising coaligned dipoles is clearly directed from donor to acceptor at each chromophore. Thus, rather than proposing a zwitterionic state for the molecules in this model system, we by contrast predict an extremely nonpolar resonance form tending toward the ideal quinonoidal form.

As a final note, we remark that our DFT calculation of a monolayer on quartz gives essentially identical results to those obtained for the multilayer described in Sec. III.

[1]R. M. Metzger, Chem. Rev. **103**, 3803 (2003).
[2]R. M. Metzger, Anal. Chim. Acta **568**, 146 (2006).
[3]A. Jaiswal, D. Rajagopal, M. V. Lakshmikantham, M. P. Cava, and R. M. Metzger, Phys. Chem. Chem. Phys. **9**, 4007 (2007).
[4]B. Chen and R. M. Metzger, J. Phys. Chem. B **103**, 4447 (1999).
[5]G. J. Ashwell, J. R. Sambles, A. S. Martin, W. G. Parker, and M. Szablewski, J. Chem. Soc., Chem. Commun. **19**, 1374 (1990).
[6]A. S. Martin, J. R. Sambles, and G. J. Ashwell, Phys. Rev. Lett. **70**, 218 (1993).
[7]R. M. Metzger, B. Chen, U. Hopfner, M. V. Lakshmikantham, D. Vuillaume, T. Kawai, X. L. Wu, H. Tachibana, T. V. Hughes, H. Sakurai, J. W. Baldwin, C. Hosch, M. P. Cava, L. Brehmer, and G. J. Ashwell, J. Am. Chem. Soc. **119**, 10455 (1997).
[8]A. Broo and M. C. Zerner, Chem. Phys. **196**, 423 (1995).
[9]N. Okazaki, J. R. Sambles, M. J. Jory, and G. J. Ashwell, Appl. Phys. Lett. **81**, 2300 (2002).
[10]G. J. Ashwell, Thin Solid Films **186**, 155 (1990).
[11]G. J. Ashwell, G. Jefferies, E. J. C. Dawnay, A. P. Kuczynski, D. E. Lynch, Y. Gongda, and D. G. Bucknall, J. Mater. Chem. **5**, 975 (1995).
[12]G. J. Ashwell, E. J. C. Dawnay, A. P. Kuczynski, M. Szablewski, I. M. Sandy, M. R. Bryce, A. M. Grainger, and M. Hasan, J. Chem. Soc. Faraday Trans. **86**, 1117 (1990).
[13]G. J. Ashwell, A. Chwialkowska, and L. R. H. High, J. Mater. Chem. **14**, 2389 (2004).
[14]J. W. Baldwin, B. Chen, S. C. Street, V. V. Konovalov, H. Sakurai, T. V. Hughes, C. S. Simpson, M. V. Lakshmikantham, M. P. Cava, L. D. Kispert, and R. M. Metzger, J. Phys. Chem. B **103**, 4269 (1999).
[15]A. Honciuc, A. Otsuka, Y. H. Wang, S. K. McElwee, S. A. Woski, G. Saito, and R. M. Metzger, J. Phys. Chem. B **110**, 15085 (2006).
[16]M. Pickholz and M. C. dos Santos, J. Mol. Struct.: THEOCHEM **432**, 89 (1998).
[17]F. Terenziani, A. Painelli, A. Girlando, and R. M. Metzger, J. Phys. Chem. B **108**, 10743 (2004).
[18]F. Terenziani and A. Painelli, Phys. Rev. B **68**, 165405 (2003).
[19]A. Painelli, Chem. Phys. Lett. **285**, 352 (1998).
[20]A. Painelli, Chem. Phys. **245**, 185 (1999).
[21]S. J. Clark, M. D. Segall, C. J. Pickard, P. J. Hasnip, M. J. Probert, K. Refson, and M. C. Payne, Z. Kristallogr. **220**, 567 (2005).
[22]M. D. Segall, P. J. D. Lindan, M. J. Probert, C. J. Pickard, P. J. Hasnip, S. J. Clark, and M. C. Payne, J. Phys. Condens. Matter **14**, 2717 (2002).
[23]B. G. Pfrommer, M. Cote, S. G. Louie, and M. L. Cohen, J. Comput. Phys. **131**, 233 (1997).
[24]The only published crystal structures available for comparisons are of the "α" variants (denoting the position of the hetero-atom in the aromatic ring system).
[25]R. M. Metzger, N. E. Heimer, and G. J. Ashwell, Mol. Cryst. Liq. Cryst. **107**, 133 (1984).
[26]N. A. Bell, C. S. Bradley, R. A. Broughton, S. J. Coles, D. E. Hibbs, M. B. Hursthouse, A. K. Ray, D. J. Simmonds, and S. C. Thorpe, J. Mater. Chem. **15**, 1437 (2005).
[27]T. Xu, T. A. Morris, G. J. Szulczewski, R. R. Amaresh, Y. L. Gao, S. C. Street, L. D. Kispert, R. M. Metzger, and F. Terenziani, J. Phys. Chem. B **106**, 10374 (2002).
[28]G. J. Ashwell and G. A. N. Paxton, Aust. J. Chem. **55**, 199 (2002).
[29]J. P. Perdew, K. Burke, and M. Ernzerhof, Phys. Rev. Lett. **77**, 3865 (1996).
[30]S. J. Clark and J. Robertson, Phys. Rev. B **82**, 085208 (2010).